ELSEVIER

Synthetic Metals 101 (1999) 281–284

SYNTHETIC METALS

Ultrafast Spectroscopic Holography in Conjugated Polymers

B. Kraabel[a], D. McBranch[a], B. Hsieh[b], F. Wudl[c]

[a]Los Alamos National Laboratory, MS J-585, Los Alamos, NM 87545, U.S.A.
[b]Xerox Corporation, 800 Phillips Rd., Webster, NY 14580, U.S.A.
[c]Institute for Exotic Materials, University of California, Los Angeles, CA 90095, U.S.A.

Abstract

We present a detailed study of femtosecond transient holography in conjugated polymers and blends, using tunable non-degenerate four-wave mixing. Combined with spectral transient absorption studies, these experiments determine the complex photoinduced index of refraction over the photon energy range from 1-2.5 eV. By performing a Kramers-Kronig transformation of the broad-band photoinduced absorption spectrum, a reliable spectrum of the diffraction efficiency can be obtained. The samples used include luminescent polymers from the poly-phenylene-vinylene (PPV) family, as well as charge transfer blends of PPV's with soluble methanofullerenes. One can achieve diffraction efficiencies on the order of one percent for a single femtosecond pulse, and by controlling the degree of charge transfer it is possible to tune the time constant over the range from 1 to 100 ps. These materials represent a potential holographic information processing density up to 12 orders of magnitude higher than other holographic nonlinear optical materials.

Keywords: femtosecond, holography, polymer, charge transfer

1. Introduction

Holographic gratings have attracted interest for applications such as interconnection networks, 3-D optical data storage and optical computing[1]. Although the most widely studied materials have been inorganic photorefractive materials[2,3], recently organic holographic materials such as photorefractive polymers, photochromic molecules, and conjugated polymers have received increased attention[4-6]. Typically materials present a trade-off between rapid response time and high diffraction efficiency. The materials with the largest diffraction efficiencies have been photorefractives [3,7], but the response time of these materials is on the time scale of seconds. Third order nonlinear optical materials have essentially instantaneous response times, but are plagued by low diffraction efficiencies. Conjugated polymers provide a unique class of materials which combine fast response times (subpicosecond) with high diffraction efficiencies [8]. In addition, the response time of these materials can be tuned from picoseconds to hundreds of picoseconds by blending them with electron acceptors such as C_{60}.

We investigated the diffraction efficiency of poly(2,3-diphenyl-5-hexyl-p-phenylene vinylene) (DP-PPV) and of DP-PPV and poly[2-methoxy,5-(2'-ethylhexoxy)-1,4-phenylene vinylene] (MEH-PPV) blended with cholestanoxy methanofullerene (C_{60}) [15] over a wide spectral range using non-degenerate four-wave mixing. The PPV samples were spun cast in an inert atmosphere and held under a dynamic vacuum of 10^{-5} mBar for the duration of the experiment in order to prevent photo-oxidation. In order to compare the results with those previously published we use the temporal diffraction efficiency (TDE) as a figure-of-merit. The TDE is defined as η/τ, where η is the diffraction efficiency and τ is the time constant governing the holographic buildup.

2. Experiment

The experimental setup used is similar to that described in ref. 8. However, in order to generate probe pulses that could be tuned over a large frequency range we used an IR-pumped optical parametric amplifier (OPA). The output of the OPA is two pulse trains with distinct wavelengths. The shorter wavelength pulse train, (signal beam), spans the range from 1200 nm to 1600 nm, and the longer wavelength pulse train (idler), spans the range from 1600 nm to 2600 nm. By mixing the signal or idler with the 810 nm fundamental in a BBO crystal we generated pulses spanning the range from 480 nm to 620 nm. To cover the range from 600 nm to 750 nm we doubled the signal (again using a BBO crystal), and to cover the range from 850 nm to 1150 nm we doubled the idler. These pulses were then used as probe

PII: S0379-6779(98)00370-1

pulses to measure the diffraction efficiency of a transient holographic grating.

The transient holographic grating was created by pumping the sample with two 405 nm pump pulses which crossed at an angle of 11 degrees at the sample plane. Through interference these pulses create an intensity pattern on the sample which leads to a population grating. Due to the large nonlinearities of conjugated polymers, the photoexcitations strongly modulate the complex index of refraction over a broad spectral range.

The probe beam was incident on the sample at 6 degrees as measured from the sample normal. In order to compare the results at different probe wavelengths, care was taken to monitor the incident pump fluence and the incident probe fluence for all measurements. This was done using beamsplitters to send a pump reference beam and a probe reference beam into two separate photodetectors. The transmitted probe beam (or diffracted probe beam) was measured with a third photodetector. Using a boxcar integrator, we normalized each diffracted probe pulse to the incident pump fluence, the incident probe fluence and the transmitted probe fluence. Spurious signals due to scattering and luminescence were taken into account by measuring the signal at negative delay times (i.e. the probe pulse arrives prior to the pump pulses) and by subtracting this baseline from the signal at positive delay times.

The PA experiments were conducted using the optimized transient absorption setup described previously [9]. Only one pump beam was used for these experiements. The wavelength range of the PA measurements was extended using the output of the IR-pumped OPA for the probe.

3. Results and Discussion

In order to relate the diffraction effiency to the complex index of refraction the following conditions should be met [3]:

$$qw \gg 1, \quad (1)$$

$$z_0/d \gg 1, \quad (2)$$

$$\alpha d \ll 1, \quad (3)$$

$$\Delta N/N \ll 1. \quad (4)$$

In equation (1) q is the grating wavevector and w is the width of the interaction zone of the pump beams. In our measurements $q \approx 3$ μm^{-1} and $w \geq 400$ μm. Equation (2) stipulates that the overlap length z_0 of the two pump beams in the z direction (normal to the sample plane) must be large compared to the sample thickness, d, which is satisfied since $d \leq 1$ μm. The requirement of equation (3), where αd represents the linear absorption of the pump pulses, was the least stringently met since low absorption translated to smaller signals. For the sample used in our measurement $\alpha d = 1$ at the pump wavelength. However, we will show below that this does not invalidate our results. Finally, the inequality of equation (4) (ΔN is the photoinduced change in the complex index of refraction N) is satisfied since ΔN/N was of order 0.1.

Under these conditions the diffraction efficiency, η, is related to ΔN in the following manner [3]:

$$\eta \equiv \frac{I_D}{I_0} = \left|\frac{\pi \Delta N d}{\lambda}\right|^2 = \left(\frac{\pi \Delta n}{\lambda}\right)^2 + \left(\frac{\Delta \alpha d}{4}\right)^2, \quad (5)$$

where I_D is the diffracted probe intensity, I_0 is the incident probe intensity, λ is the wavelength of the probe pulse, Δn is the change in the real part of the refractive index and the other symbols have the same meaning as above. Hence by measuring the diffraction efficiency (η) and the PA ($\Delta \alpha d$) we can access the change in the real part of the refractive index (Δn).

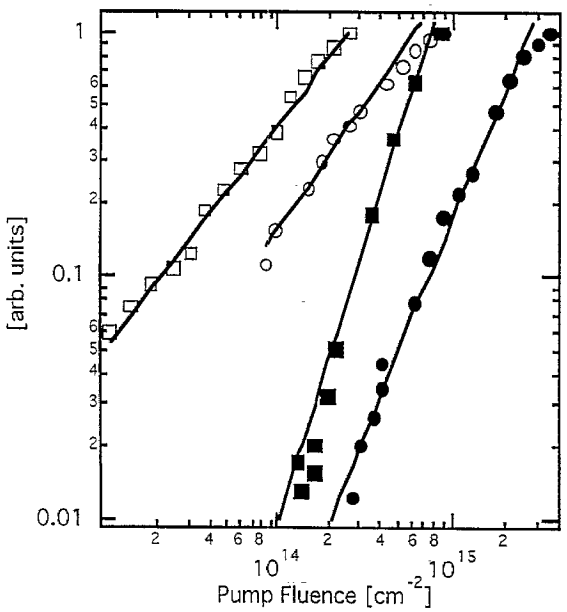

Fig. 1. The open squares (circles) show dependence of the PA at on pump fluence at 500 (850) nm for DP-PPV. The solid line is a fit with to $I^{0.9}$ (I^1), where I represents the pump fluence. The solid squares (circles) represent the dependence of the diffraction efficiency at 500 (850) nm, and the solid line is a fit to $I^{2.3}$ ($I^{1.8}$).

In Fig. 1 we show the intensity dependence of the PA and of the diffracted signal at wavelengths of 500 nm and 850 nm for DP-PPV. The pump fluence for the diffraction efficiency is calculated taking into account the coherent sum of the two pump beams. Thus the fluence noted on the abscissa of Fig. 1 corresponds to the pump fluence in the regions where the pump beams interfered constructively. The curves show that the diffracted signal has a quadratic dependence on the pump fluence, while the PA depends linearly on pump fluence. This relation holds up until saturation, which occurs at a pump fluence of approximately 10^{15} cm^{-2}. The measurements of the diffraction efficiency that we report below were

taken just beneath this saturation limit, at a pump fluence of 7 X 10^{14} cm^{-2}.

Equation (5) implies that the η should follow the square of the complex index of refraction. From the quadratic relationship between the PA and η seen in Fig. 1 we feel confident that we are indeed operating in the regime governed by equation (5).

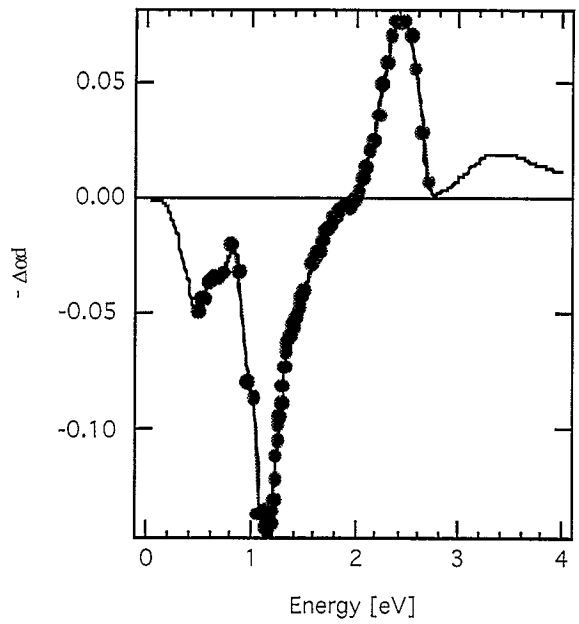

Fig. 3. The solid dots show the PA spectrum of DP-PPV, and the solid line shows the spectrum extended as described in the text. The pump fluence was 7 X10^{14} cm^{-2}.

Figure 3 shows the chirp-free PA spectrum for DP-PPV at a delay time corresponding to the signal maximum and at a pump fluence of 7 X 10^{14} cm^{-2}. The spectrum consists of a strong PA feature at 1.24 eV (1 μm), and a weaker one peaking in the IR around 0.5 eV (2.5 μm), along with a strong stimulated emission (SE) band centered around 2.5 eV (500 nm). In order to perform the Kramers-Kronig (KK) transformation on this spectrum, we first extended the IR PA feature farther into the IR by assuming it has a Gaussian lineshape. We note here that previous work has detected the low-energy side of this PA feature in PPV[10],and indicated that the peak of this feature was at or above 0.5 eV. Since in our measurement we find that the peak is at or below 0.5 eV, we feel justified in fitting it to a Gaussian peaking at 0.5 eV. To take into account the bleaching of the linear absorption, we scaled the linear absorption and added it to the PA spectrum so that the integral of the entire PA spectrum was zero. This ensures that oscillator strength is conserved. The PA spectrum extended in this way is shown in Fig.3 as the solid curve.

Taking the KK transform of the extended PA spectrum of Fig. 3 we calculated the spectrum of the diffraction efficiency using equation 5 in order to compare it with the measured diffraction efficiency. This is shown in Fig. 4. Clearly, there is an excellent agreement between the spectrum obtained from the KK analysis of the PA spectrum and the directly measured diffraction spectrum. We thus feel confident the broad-band PA spectrum may be used in order to calculate the diffraction efficiency, under the conditions stipulated by equations (1) to (4).

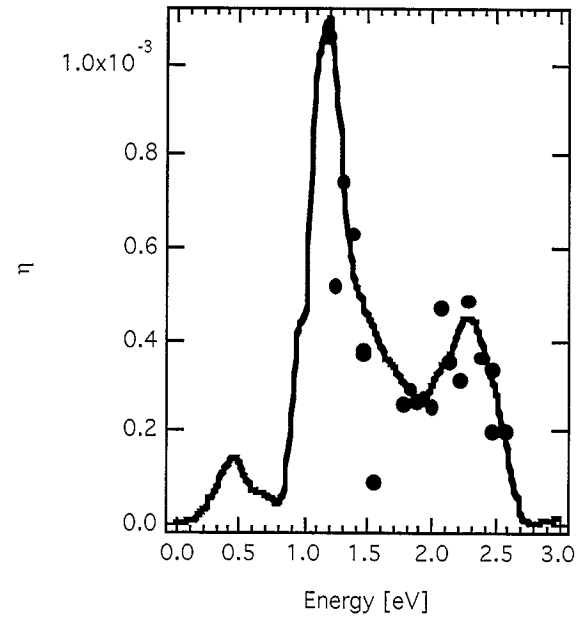

Fig. 4. The solid curve represents the diffraction efficiency as calculated from equation (5) and using the KK transformation of the data in Fig. 3. The solid circles show the measured diffraction efficiency. The pump fluence was 7 X 10^{14} cm^{-2}.

Fig. 5 shows the diffraction efficiency for a thick sample ($\alpha d \approx 2$) of DP-PPV/C_{60} (1:1). The solid squares correspond to the measured diffraction efficiency, while the heavy line shows the photoinduced change in the real part of the index of refraction(Δn), scaled to correspond to the first term in equation (5). This curve was calculated by performing a KK transform on the broad-band PA of this sample, as described above for the DP-PPV sample. The thin solid line in Fig. 5 corresponds to the calculated diffraction spectrum, again using equation (5) and the KK transform of the PA spectrum. The measured diffraction efficiency corresponds much more closely with the first term in equation (5) (i.e. Δn) than with the sum of the two terms.

As can be seen by comparing Figs. 5 and 4, the PA spectrum at zero delay time (i.e. at the maximum of the signal) for pristine DP-PPV is similar to that observed for the blend DP-PPV/C_{60} (1:1). This is in contrast to what has been observed for other PPV/C_{60} and P3OT/C_{60} blends, where a marked change in the PA spectrum was observed upon adding fullerenes to the polymer host [11,12]. This indicates that in DP-PPV charge transfer is not an efficient, ultrafast process, as it is in these other blends. This is supported by the data of Fig. 6. Curves (a) and (b) represent the dynamics at 810 nm of MEH-

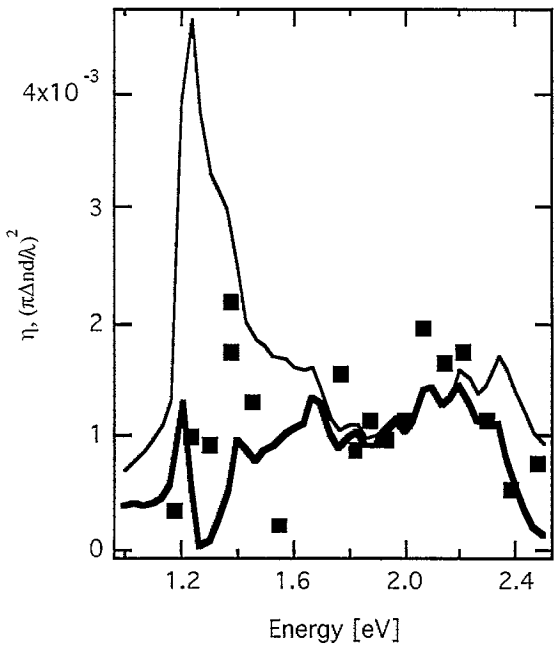

Fig. 5. The thin solid line shows the diffraction spectrum calculated from the KK transform of the PA spectrum of DP-PPV/C_{60} (1:1). The heavy solid line shows the photoinduced change in the real part of the index of refraction, scaled to correspond to the first term in equation (5). The solid squares correspond to the measured diffraction efficiency for the same sample. The pump fluence was 7 X 10^{14} cm^{-2}.

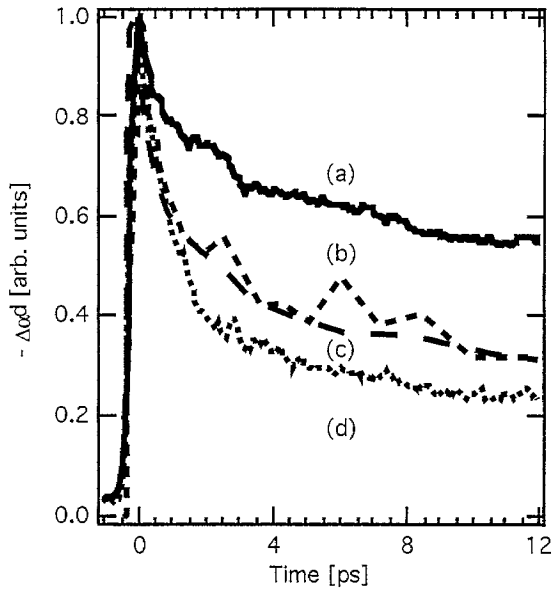

Fig. 6. Dynamics of (a) MEH-PPV/C_{60} (4:1) and (d) MEH-PPV at 810 nm upon pumping at 405 nm (6X10^{14} cm^{-2}). Curves (b) and (c) show the dynamics of DP-PPV (10^{15} cm^{-2}) and DP-PPV/C_{60} (1:1) (3X10^{14} cm^{-2}) at 780 nm and 700 nm, respectively, upon pumping at 405 nm .

PPV/C_{60} (4:1) and of pristine MEH-PPV, respectively. Curves (c) and (d) are for pristine DP-PPV and DP-PPV/C_{60} (1:1) at 1 μm. Clearly the dynamics of the PA are much slower upon adding 25% C_{60} to MEH-PPV, which is indicative of metastable charge transfer. However, the dynamics of the DP-PPV are virtually unchanged upon adding 100% C_{60}, supporting the conclusion that charge transfer in this polymer host is not as effective.

Finally we note that the maximum diffraction efficiency we obtained was 1% for a thick ($\alpha d > 6$) film of DP-PPV, which is similar to what was observed in MEH-PPV [8]. This occurs at a wavelength of approximately 900 nm. This gives a TDE of 0.01/10^{-13} s = 10^{11} s^{-1}. This is two orders of magnitude larger than that reported for other third-order nonlinear polymer experiments, 11 orders of magnitude larger than the best photorefractives, and 12 orders of magnitude larger than results reported for photo-isomerization.[13,14].

4. References

[1] P. Günter, and J.-P. Huignard, *Photorefractive Materials and Their Applications* (Springer-Verlag, NY, 1988).

[2] E.S. Maniloff and K.M. Johnson, J. Appl. Phys. **70**, 4702 (1991).

[3] H. Eichler, P. Günter and D. Pohl, *Laser-Induced Dynamic Gratings* (Springer-Verlag, NY, 1986).

[4] C. Halvorson, A. Hays, B. Kraabel, R. Wu, F. Wudl and A.J. Heeger, Science **265**, 1215 (1994).

[5] W.E. Moerner and S.M. Silence, Chem. Revs. **94**, 127 (1994).

[6] J. Xu, G. Zhang, Q. Wu, Y. Liang, S. Liu, Q. Sun, X. Chen and Y. Shen, Opt. Lett. 20, 504 (1995).

[7] B. Volodin, Sandalphon, K. Meerholz, B. Kippelen, N. Kukhtarev and N. Peygambarian, Opt. Eng. **34**, 2213 (1995).

[8] E.S. Maniloff, D. Vacar, D.W. McBranch, H.L. Wang, B.R. Mattes, J. Gao and A.J. Heeger, Opt. Comm. **141**, 243 (1997).

[9] V. Klimov and D.W. McBranch, Opt. Lett. **23**, 277 (1998).

[10] J.W.P. Hsu, M. Yan, T.M. Jedju and L.J. Rothberg, Phys. Rev. B **49**, 712 (1993).

[11] B. Kraabel, D.W. McBranch, L. Smilowitz, C.H. Lee, K. Lee, N.S. Sariciftci, D. Moses and A.J. Heeger, *Recent Advances in the Chemistry and Physics of Fullerenes and Related Materials* (Electrochemical Society, Inc., Pedington, NJ, 1994).

[12] B. Kraabel, J.C. Hummelen, D. Vacar, D. Moses, N.S. Sariciftci, A.J. Heeger and F. Wudl, J. Chem. Phys. **104**, 4267 (1996).

[13] V. Pham, G. Manivannan, R. Lessard and R. Po, Opt. Mat. **4**, 467 (1995).

[14] J. Zhao, F. Dong, H. Qu, P. Ye, X. Fu, L. Qiu and Y. Shen, Appl. Phys. B **61**, 377 (1995).

[15] J.C. Hummelen, B.W. Knight, F. Lepeq, F. Wudl, J. Yao, C.L. Wilkins, J. Org. Chem. **60**, 532 (1995).